Langmuir

Article

pubs.acs.org/Langmuir

Antibacterial Activity of Glutathione-Coated Silver Nanoparticles against Gram Positive and Gram Negative Bacteria

Angelo Taglietti,*[,†] Yuri A. Diaz Fernandez,*[,†] Elvio Amato,[†] Lucia Cucca,[†] Giacomo Dacarro,[‡] Pietro Grisoli,[§] Vittorio Necchi,[∥] Piersandro Pallavicini,[†] Luca Pasotti,[†] and Maddalena Patrini[‡]

[†]Dipartimento di Chimica, Sezione di Chimica Generale, Università di Pavia, viale Taramelli, 12 - 27100 Pavia, Italy

[‡]Dipartimento di Fisica "A. Volta", Università di Pavia, Via Bassi, 6 - 27100 Pavia, Italy

[§]Dipartimento di Scienze del Farmaco, Università di Pavia, viale Taramelli, 10 - 27100 Pavia, Italy

[∥]Centro Grandi Strumenti, Università di Pavia, Via Bassi 21 - 27100 Pavia, Italy

Supporting Information

ABSTRACT: In the present paper, we study the mechanism of antibacterial activity of glutathione (GSH) coated silver nanoparticles (Ag NPs) on model Gram negative and Gram positive bacterial strains. Interference in bacterial cell replication is observed for both cellular strains when exposed to GSH stabilized colloidal silver in solution, and microbicidal activity was studied when GSH coated Ag NPs are (i) dispersed in colloidal suspensions or (ii) grafted on thiol-functionalized glass surfaces. The obtained results confirm that the effect of dispersed GSH capped Ag NPs (GSH Ag NPs) on *Escherichia coli* is more intense because it can be associated with the penetration of the colloid into the cytoplasm, with the subsequent local interaction of silver with cell components causing damages to the cells. Conversely, for *Staphylococcus aureus*, since the thick peptidoglycan layer of the cell wall prevents the penetration of the NPs inside the cytoplasm, the antimicrobial effect is limited and seems related to the interaction with the bacterial surfaces. Experiments on GSH Ag NPs grafted on glass allowed us to elucidate more precisely the antibacterial mechanism, showing that the action is reduced because of GSH coating and the limitation of the translational freedom of NPs.

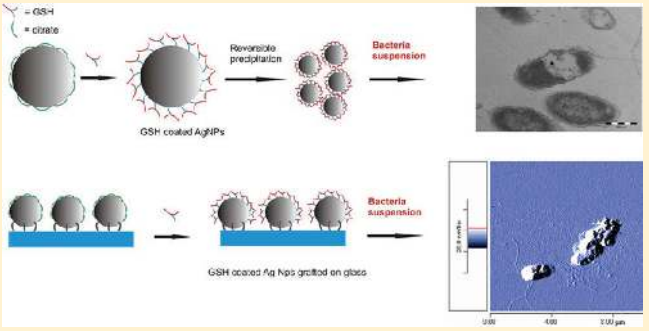

INTRODUCTION

The use of silver nanoparticles (Ag NPs) as antibacterial agents has become very important in recent years,[1−8] following the well-known use of silver ions as an antibacterial agent. The well-established microbicidal action of silver ions, which has been exploited since ancient times,[9,10] is universally considered to be a result of (i) Ag^+ interactions with cysteine in critical regions of proteins and other cell constituents (ii) causing K^+ loss from the membrane, with disruption of cellular transport systems (iii) causing damage in respiration, (iv) perturbation of cellular growth, and (v) interaction with DNA.[11] Moreover, in low concentration, silver is not toxic to human cells, and hence it can be considered an environmentally friendly antimicrobial, also considering the weak ability of bacteria to develop resistance toward silver ions,[12,13] even if some examples of resistant bacterial strains have been reported.[14] In this approach, Ag NPs have antibacterial action not only relying on Ag^+ release, which could offer a real alternative for the future of antimicrobial treatments.

The scientific debate on the mechanism for the antibacterial effect of Ag NPs is still open.[2,4,15−17] Some authors have suggested that the effect should rely mainly on release of silver ions from NPs surfaces, followed by the interaction of Ag^+ with the cellular targets.[18−20] It sounds evident that nanosilver should be more active than a similar bulk amount of silver. The ability of Ag NPs to reach bacteria proximity and a high surface/mass ratio can produce a high concentration of Ag^+ in cell surroundings, causing high microbicidal effects.[21] Nevertheless, there is evidence that Ag NP toxicity may arise from direct physical processes caused by nano-objects, like disruption of cell membrane and penetration of NPs into the cytoplasm,[2,4,15,16,23] DNA binding, or interaction with bacterial ribosome.[24] These mechanisms have been observed mainly for Gram negative bacteria, because of the low resistance of the cellular membranes, compared with the peptidoglycan rigid cellular walls of Gram positive bacteria. Recently, evidence of internalization of Ag NPs in *Staphylococcus aureus* cytoplasm has been given.[23b] The size-dependent interaction of silver nanoparticles with Gram-negative bacteria and the biological activity of silver nanoparticles as a function of the particle shape have also been investigated.[12]

Received: January 26, 2012
Revised: March 12, 2012
Published: April 30, 2012

ACS Publications © 2012 American Chemical Society

dx.doi.org/10.1021/la3003838 | *Langmuir* 2012, 28, 8140−8148

Scheme 1. LbL Approach for the Preparation of Glass Samples Functionalized with GSH Coated Ag NPs

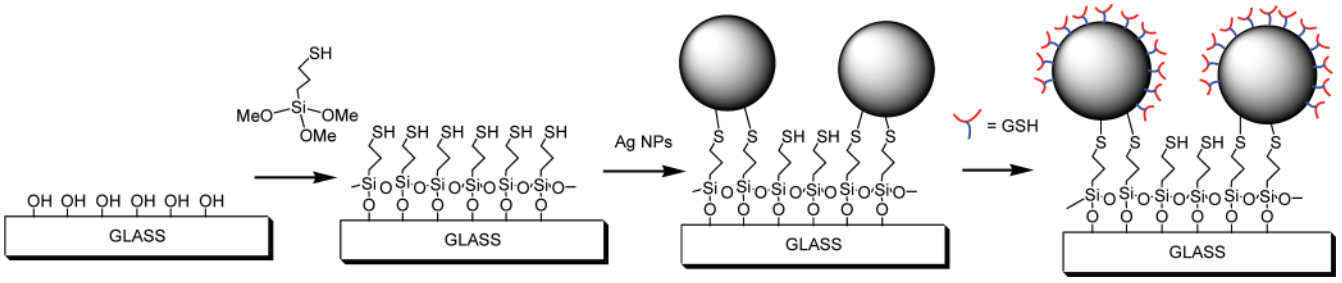

This kind of biological application for Ag NPs requires the appropriate coating of NPs surface, to avoid aggregation in highly saline media. It has been also suggested that decoration of NP surface with a biomimetic motif could favor interactions with biosystems[21,25] and enhance the solubility in water-based environments.

We have recently reported[26] that glutathione (GSH) is an ideal candidate for this purpose since this biomolecule displays a thiolic function, capable of being anchored to silver surfaces,[27] and three pH-dependent, charged functional groups (carboxylates and amine), that promote water solubility and interactions toward more complex biostructures.[28−30] The procedure developed allows the coating of already synthesized NPs, followed by purification and redissolution under physiological conditions. These biomimetically coated NPs have been well characterized, and showed a good antibacterial effect. Since NP dimensions are important for antibacterial activity,[31,32] the described method has the advantage of using postcapping of NPs with specific dimensions and shape, maintaining the original morphology.

In the present work, we report further investigation on the action of these colloidal nanoparticles, based on the comparison between the antibacterial activity of the dispersed colloid and of similar silver NPs grafted on glass surfaces, prepared by modifying a successful synthetic protocol recently developed which is based on a layer-by-layer approach[33,34] (Scheme 1). As already cited, the mechanism of antibacterial action of AgNPs is not fully understood. According to a very recent and exhaustive review,[15b] three possible mechanism are usually proposed: (i) gradual release of silver ions, which then affects DNA replication and ATP production, (ii) direct damage to cell membranes by Ag NPs, or (iii) generation of reactive oxygen species from Ag NPs and Ag^+. In our opinion, comparison between the activity of dispersed and grafted Ag NPs of similar nature could give some hints in order to better understand the mechanism of antibacterial action of AgNPs.

Our interest in monolayers of Ag NPs grafted onto glass is also due to the fact that these kinds of materials can be exploited to prepare surfaces with a significant disinfectant capability and which could be applied to prepare smart biomedical devices.[8e,f,35]

EXPERIMENTAL SECTION

Materials. Silver nitrate (>99.8%), sodium borohydride (≥99.0%), sodium citrate (>99.0%), L-glutathione reduced (99%), (3-mercaptopropyl)-trimethoxysilane (95%), and phosphate buffered saline, PBS (pH = 7.4), were purchased from Sigma-Aldrich. Iso-Sensitest Broth (ISB) and Tryptone Soya Broth (TSB) for bacterial culture were purchased from Oxoid, England. *Staphylococcus aureus* ATCC 6538 and *Escherichia coli* ATCC 10536 bacterial strains were used. Microscopy cover glass slides 24 × 24 mm^2 were purchased from Forlab (Carlo Erba).

All reagents were used as received. Water was deionized and bidistilled. Glassware was carefully cleaned with aqua regia, and then washed several times with bidistilled water under sonication before use. Citrate-capped NPs, GSH-capped NPs, and monolayers of citrate-capped silver NPs on glass were synthesized using procedures previously described.[26,33]

Preparation and Characterization of GSH-Capped NPs Monolayers on Glass. Monolayers of biomimetic coated NPs grafted on glass slides were prepared by dipping the previously described glass slides functionalized with native colloidal Ag NPs[33] in solutions of glutathione of various concentration (from 10^{-8} to 10^{-3} M) for different times ranging from 5 to 20 min. NP functionalized substrates were characterized by means of UV−vis spectroscopy and tapping-mode atomic force microscopy (Auto Probe CP Research Thermomicroscopes instrument). Absorbance UV−vis spectra were taken with a Varian Cary 100 spectrophotometer in the 300−700 nm range. Spectra of NP-functionalized glasses, showing the typical LSPR absorption, were obtained by placing the glasses on the apparatus equipped with a dedicated Varian solid sample holder. Silver content was assayed after etching the functionalized surfaces dipping them overnight in ultrapure concentrated nitric acid diluted 1:5 with water. The etching solution was analyzed by inductively coupled plasma optical emission spectrometry (ICP-OES Optima 3300 DV, Perkin-Elmer). For the release of Ag^+ from NPs-functionalized glasses, two slides were immersed in 2 mL of bidistilled water and shaken for 24 h. This time interval was chosen as 24 h is the maximum contact time considered for the proposed ME test. The silver content in the solutions was evaluated using a Shimadzu atomic absorption spectrophotometer AA-6601G, equipped with graphite-oven atomizer.

Bacterial Culture and ME Experiments. The effect of GSH capped NPs and silver ions (as silver nitrate) in disperse solution and GSH coated NPs monolayers grafted on glass surfaces was evaluated against *Staphylococcus aureus* and *Escherichia coli*. The experiments on microbicidal effect (ME)[36] on functionalized glasses were performed using a procedure described in the literature.[26,33]

Briefly, the microorganisms were grown overnight in Tryptone Soya Broth at 37 °C. Washed cells were resuspended in Dulbecco's PBS and optical density (OD) was adjusted to 0.1, corresponding approximately to 1 × 10^8 colony forming units (CFU) /ml at 650 nm wavelength. Ten microliters of bacterial suspension was deposited on a standard glass slide (76 × 26 mm^2), then the microbial suspension was covered with a glass slide (24 × 24 mm^2) functionalized with the GSH coated Ag NPs SAM, forming a thin film between the slides that facilitates direct contact of the microorganisms with the active NP surface. The two assembled glasses were introduced in a Falcon test tube (50 mL) containing 1 mL of PBS to maintain a damp environment. For each bacterial strain, two equivalent modified glasses were prepared; the slides were maintained in contact with the liquid films containing bacteria at room temperature for 5 and 24 h, respectively; for each time of contact, an unmodified glass slide was treated in the same way as the control sample. After the times of contact, 9 mL of PBS was introduced in each Falcon test tube under gentle shaking to detach the assembled glass slides. Bacterial suspensions were then grown in Tryptone Soya Agar (Oxoid;

dx.doi.org/10.1021/la3003838 | Langmuir 2012, 28, 8140−8148

Basingstoke, Hampshire, England) to count viable cells. The decimal-log reduction rate, microbicidal effect (ME), was calculated using the formula: ME = log NC − log NE (NC being the number of CFU/mL developed on the unmodified control glasses, and NE the number of CFU/mL counted after exposure to modified glasses). In other words, higher ME values correspond to a lower number of bacteria surviving in modified glasses than in control samples, and thus to a better biocidal activity. The results expressed as ME represent the average of three equivalent determinations.

For the assays on disperse solutions, the microorganisms were grown overnight in Tryptone Soya Broth at 37 °C. Washed cells were resuspended in Dulbecco's PBS and optical density (OD) was adjusted to 0.1 at 650 nm wavelength corresponding approximately to 1×10^8 colony forming units/mL (CFU/mL).

TEM Imaging and Microanalysis. TEM images at different magnifications were obtained from colloidal solutions of citrate-capped Ag NPs, and from solutions of particles coated with GSH and cysteine. After dilution ten times with bidistilled water, 10 μL drops were deposited on nickel grids (300 mesh) covered with a Parlodion membrane and observed with a Jeol JEM-1200 EX II instrument.

For the preparation of the TEM bacterial samples, we followed the procedure described for the antibacterial activity tests.[26] Samples incubated in ISB for 24 h at 37 °C with GSH Ag NPs and with silver nitrate were prepared in the presence of one-half of the minimum inhibitory concentrations (MIC_s) determined in each case to produce a sufficiently big bacterial pellet that could be manipulated in subsequent preparation steps. The MIC values were previously found[26] to be as follows: (i) for GSH Ag NPs, 180 μg/mL and 15 μg/mL for *S. aureus* and *E. coli*, respectively; (ii) for silver nitrate, 15 μg/mL and 10 μg/mL for *S. aureus* and for *E. coli*, respectively. Control samples were prepared without adding silver nitrate or colloidal silver.

Bacterial pellets harvested from both cultures were washed twice with cacodylate buffer (pH = 7.3), fixed in 2.5% glutaraldehyde and 2% paraformaldehyde in cacodylate buffer for 40 min at 4 °C, post-fixed in 1% osmium tetraoxide for 1 h at room temperature and embedded in Epon-Araldite resin mixture, and then cut with Reichert Ultracut's Leica. The sections were stained with uranyl/lead before electron microscopy investigation. The quantitative analysis of the TEM images was performed on 10 different fields for each sample, having cross sections varying from 150 to 250 μm^2. The total number of cells counted per field varied from 50 to 200 cells. The observed cells were classified in three categories: damaged, in replication, and normal cells. The percent of each category was calculated within the field and the reported value was the average of the 10 fields investigated for each sample.

Unstained sections were analyzed by electron spectroscopy imaging (ESI) using a LEO 912AB electron microscope as described by Pezzati et al.[39]

AFM on Bacteria Deposited on Functionalized Glass Slides. The microorganisms were grown overnight in Tryptone Soya Broth at 37 °C. Washed cells were resuspended in distilled water and optical density (OD) was adjusted to 0.1 at 600 nm wavelength corresponding approximately to 1×10^8 colony forming units/mL (CFU/mL). A drop of bacterial suspension (10 μL) was deposited on clean or functionalized glass slides and left in contact for 5 and 24 h in a damp environment. The drop was removed by spinning the substrate on a spin coater (spinning for 30 s at 2000 rpm), and AFM imaging was immediately performed on the substrate.

AFM images were taken from an Auto Probe CP Research Thermomicroscopes scanning system operated in tapping mode, using a Si probe with a theoretical spring constant k = 0.35−6.1 N m^{-1} (NSG03 probes from NT-MDT). Images were analyzed using *Image Processing 2.1* provided by Thermomicroscopes.

RESULTS AND DISCUSSION

Interaction of Bacteria with GSH Coated NPs in Disperse Solution. In a previous work,[26] the evaluation of minimum inhibitory concentrations (MICs) of dispersed GSH capped NPs on *Staphylococcus aureus* and *Escherichia coli*, revealed a surprisingly large difference of sensibility between these two model bacteria strains. MICs values for GSH Ag NPs were 180 μg/mL and 15 μg/mL for *S. aureus* and *E. coli*, respectively, referred as the total concentration of silver. Control experiments using silver nitrate instead of colloidal silver gave MICs of 15 μg/mL and 10 μg/mL for *S. aureus* and for *E. coli*, respectively. It is also interesting to note that for *E. coli* the MIC values for colloidal and ionic silver were very similar, while for *S. aureus* the MIC of the NPs is 1 order of magnitude greater than the MIC for ionic silver. Thus, it sounded obvious that the difference in MICs obtained with GSH Ag NPs had to be ascribed to a difference in the interactions between Ag NPs and different (Gram positive and Gram negative) bacteria.[26] To investigate this interaction, we decided to perform a TEM characterization of bacteria cultures exposed to GSH Ag NPs and to completely ionized silver (i.e., silver nitrate), in order to find additional evidence of the different effect observed. These experiments were performed using subinhibitory silver concentrations of about one-half the determined MIC in each case. The TEM images obtained showed that the NPs are present inside the cytoplasm of *E. coli*, associated with large zones of electron-translucent cytoplasm, featuring either localized or complete separation of the cell membrane from the cell wall (Figure 1a). Conversely, for *S. aureus* the NPs do not penetrate into the cellular wall, and no evident damage is observed close to the electron-dense NPs (Figure 1b, further images describing the interaction of NPs with both cell strains can be found in Supporting Information).

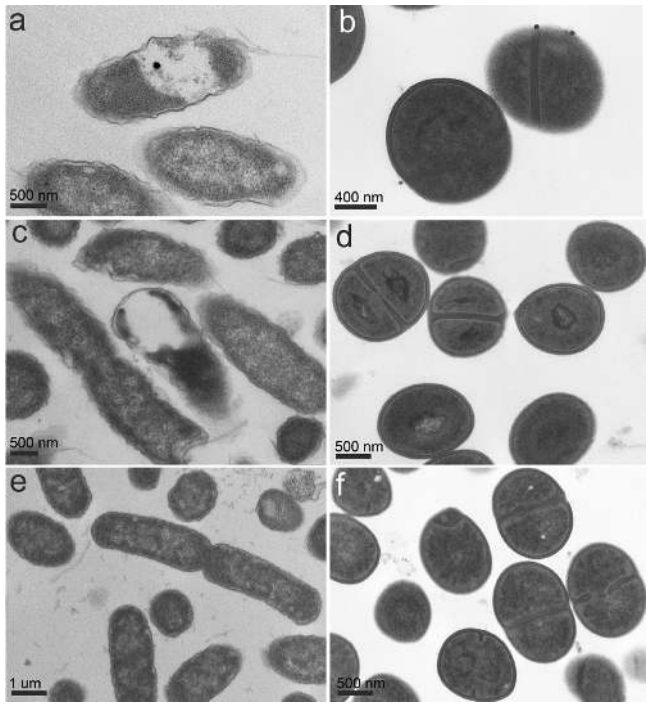

Figure 1. Morphological comparison of bacteria by TEM imaging: (a) *E. coli* treated with GSH coated NPs; (b) *S. aureus* treated with GSH coated NPs; (c) *E. coli* treated with silver nitrate; (d) *S. aureus* treated with silver nitrate; (e) *E. coli* control sample; (f) *S. aureus* control sample.

Since the quasi-spherical electron-dense objects observed attached to the cell wall or inside the cytoplasm of the bacteria had dimensions larger than the original capped NPs (7 ± 4

dx.doi.org/10.1021/la3003838 | *Langmuir* 2012, 28, 8140−8148

nm),[26] we performed microanalysis assays coupled to TEM imaging to investigate the presence of silver in these objects. These analyses demonstrated that the objects observed are formed by a core of silver, surrounded by a shell of another material (Figure 2a,b). We also prepared TEM samples without

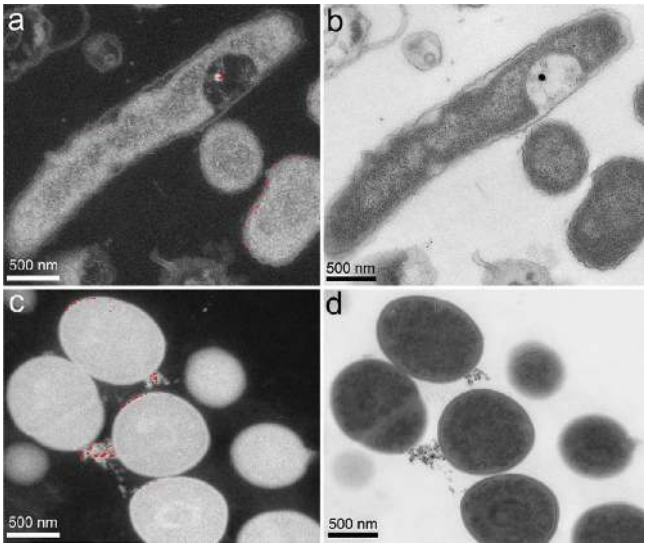

Figure 2. TEM-ESI microanalysis of bacteria incubated 24 h with GSH capped silver NPs: *E. coli* (a) silver distribution, (b) respective morphological image; *S. aureus* (c) silver distribution, (d) respective morphological image. The presence of silver is indicated by red spots.

postfixation with osmium tetraoxyde (the classical contrast agent used in TEM), and the images recorded on these samples (see Supporting Information Figure 5S) suggested that the electron-dense objects observed in the contrasted images are core−shell-like aggregates, having a heavier material inside (i.e., silver), surrounded by a less dense matrix (biological material). When the contrast agent was used, this subtle difference vanished at TEM, since OsO_4 is well-known to contrast biological phospholipidic membranes and proteins.[38] As a matter of fact, in some contrasted images the NPs are visibly attached to the cellular wall of *S. aureus*, surrounded by lighter materials, presumably of biological origin (Figure 3a,b). Massive aggregates of NPs surrounded by biological material are observed in some TEM images of *S. aureus* (Figure 3c) and less frequently in *E. coli* samples (Figure 3d). Also, during the evaluations of MICs, precipitation was reported after 24 h of incubation in *S. aureus* cultures when the concentration of NPs was sufficiently high to produce macroscopic effects. Since the GSH Ag NPs themselves are soluble, dispersed, and stable at the pH of the culture broth (pH = 7), we could presume that the precipitation and the aggregation observed are produced by the interaction of the NPs with biological material, as proposed by others authors in similar systems: the establishment of a "corona" of membrane "building elements" around highly charged Ag NPs is well-known in the literature.[4] Furthermore, comparing the TEM of NPs-treated bacteria with the control sample (bacteria incubated without silver, Figure 1e,f; see also Figure 1S and 2S in Supporting Information), we can observe that some extracellular material is present only when GSH Ag NPs are added (Figure 3a,b; see also Figure 3S and 4S in Supporting Information).

In the case of *E. coli*, the large zones of cellular damage associated to the NPs showed a local effect, once the NPs have

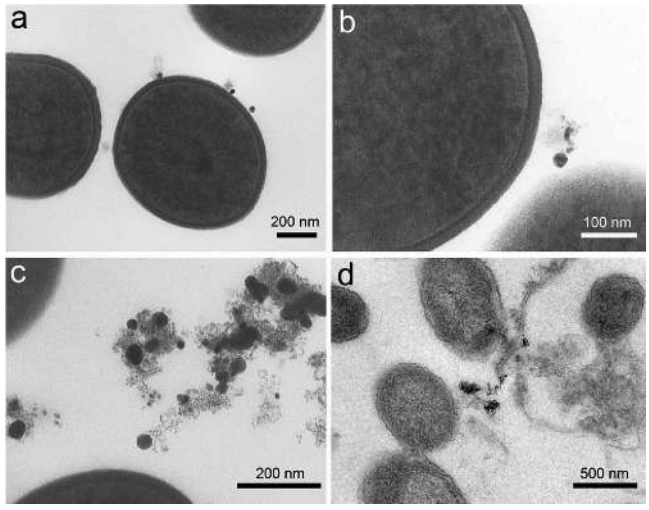

Figure 3. Interaction of GSH coated silver NPs with biological material from bacteria: (a,b) *S. aureus*, NPs attached to the cellular wall, surrounded by a lighter material presumably generated by the cells; massive aggregates composed by silver NPs and biological material observed outside the cells of (c) *S. aureus*, (d) *E. coli*.

been incorporated into the cytoplasm. The cellular material seemed to collapse around the included NP, and the cellular membrane was evidently disrupted to a large extent.[23a]

Conversely, when silver nitrate was used, no electron-dense aggregates were observed either inside or outside the cellular structures (Figure 1c,d; see also Figure 1S and 2S in Supporting Information). This result confirmed that the massive objects observed in the samples treated with NPs were not the result of Ag^+ precipitation/accumulation, but came from aggregation caused by Ag NPs.

In all the samples treated with colloidal and ionic silver, evidence of biological stress was present, as revealed by the quantitative analysis of TEM images (Table 1). More than the

Table 1. Quantitative Analysis of Bacteria Cells from TEM Images[a]

sample	% damaged	% division
E. coli control	5 ± 2	5 ± 2
E. coli AgNO3	51 ± 1	0
E. coli Ag NPs	58 ± 3	0
S. aureus control	0	28 ± 2
S. aureus $AgNO_3$	0	22 ± 1
S. aureus Ag NPs	0	7 ± 1

[a]Typically, two categories have been counted (damaged cells and cells in division) and the percent calculated under the whole population observed in the image. Examples of TEM analyzed images are reported in Figure 6Sa−f in the Supporting Information.

50% of *E. coli* cells presented broken membranes and large zones of cellular damage, compared to the control culture having only 5% of damaged cells. Particularly, in the presence of silver NPs, many *E. coli* bacteria presented the cellular membrane detached from the cytoplasm. On the other hand, no evident damage was observed either in *S. aureus* cultures treated with ionic silver or in those treated with GSH Ag NPs. For both cellular strains, GSH Ag NPs reduced the number of cells in the replication state, while ionic silver interfered only with the bacterial replication of *E. coli* under our experimental conditions. These results support the idea that our GSH-

dx.doi.org/10.1021/la3003838 | *Langmuir* 2012, 28, 8140−8148

capped nanoparticles have two different modes of action against Gram negative and Gram positive microorganisms, associated with the capacity of the NPs to penetrate inside the cytoplasm. To find further evidence of this fact, we decided to evaluate the microbicidal effect of GSH Ag NPs when they are grafted on a functionalized glass surface. When firmly grafted on a glass surface, GSH Ag NPs will have almost completely restricted translational degrees of freedom,[34,35] and cellular internalization of the NPs is not possible.

Coating of Silver NPs Self-Assembled Monolayers with Glutathione. Self-assembled monolayers of biomimetic capped nanoparticles were prepared using the layer-by-layer approach. As previously reported,[33] starting from thiol-functionalized glasses and citrate-capped silver NPs colloids (i.e., the same silver NPs used to prepare the disperse biomimetic coated NPs), we obtained a homogeneous monolayer of silver NPs firmly anchored to the surface. We have demonstrated that in the SAMs obtained by this procedure the Ag NPs are partially immersed into the grafting monolayer and present 66% of the surface exposed to the solvent.[33] Exploiting this exposed surface, we performed a coating with glutathione, in order to obtain biomimetically coated silver NPs, similar to those obtained in disperse solution, but anchored to glass surfaces.

The coating process of the grafted Ag NPs with GSH was investigated by UV–vis spectroscopy and AFM techniques. The glass microscope slides functionalized with citrate-capped silver NPs were immersed in solutions containing different amounts of GSH, and the UV–vis spectra were measured before and after immersion.

The LSPR spectra[36] of the Ag NPs anchored to the thiol-modified surface presents a maximum around 390 nm,[33] that red shifts up to 416 nm after immersion for 5 min in the solution of GSH (see Figure 4a). As can be observed, the

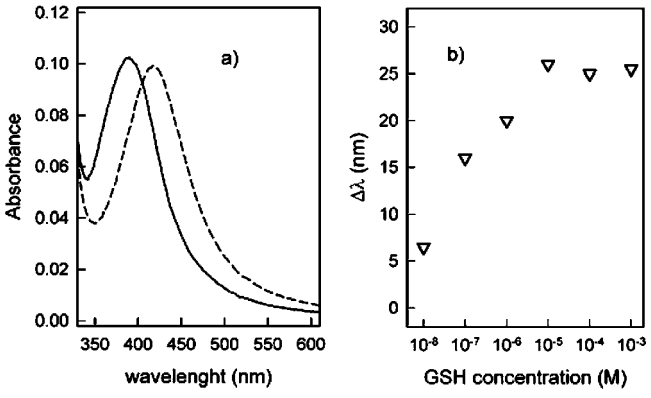

Figure 4. (a) UV–vis spectra of glass slides functionalized with SAMs of Ag NPs native (solid line) and the same after immersion in 10^{-3} M GSH for 5 min (dashed line). (b) Plot of variation of LSPR peak position of grafted Ag NPs after 5 min immersion of functionalized glass slides in GSH solutions of different concentration.

position of the maximum depends on the concentration of GSH in solution (Figure 4b). The progressive variation of the LSPR band can be ascribed to the modification of the effective refraction index experienced by the NPs, when the monolayer of GSH is formed on silver surface.[27] The profile of $\Delta\lambda$ as a function of the concentration of GSH in solution displays a plateau at 10^{-5} M (Figure 4b). Using this concentration, we performed coatings with different immersion times, and we observed that the maximum red-shift of the LSPR band was reached after a few seconds. Therefore, it is reasonable to consider that, for this concentration or higher, the coating process is complete using short immersion times. For simplicity, we adopted a coating procedure with immersion of NPs to functionalize glasses in solutions 10^{-3} M of GSH for 5 min, in order to ensure reproducibility.

AFM images of the glass slides before and after GSH coating were very similar using this functionalization procedure (see Figure 7S in Supporting Information). Furthermore, ICP-OES assays on etched samples (i.e., NP-functionalized surfaces treated with HNO_3 to oxidize silver) demonstrated that the amount of silver grafted to the surface (0.35 $\mu g/cm^2$) remains unchanged after the GSH coating process.[33] Merging these results, we can conclude that the simple coating procedure adopted here yields saturated coating layers on Ag NPs grafted to the surface and does not modify the dimension of the NPs or the surface concentration of NPs in the grafted monolayer.

Antibacterial Activity of GSH Coated Silver-NPs Grafted on Glass Surface. The antimicrobial activity of these GSH Ag NPs monolayers against *E. coli* and *S. aureus* was investigated. The procedure employed allows the evaluation of the microbicidal effect (ME) in a thin liquid film in contact with the functionalized surface.[33,36] Experimental results after 5 and 24 h showed that the glass slides functionalized with Ag NPs coated with GSH displayed a reduced bactericidal effect, compared to disperse GSH Ag NPs (Table 2). As for colloidal dispersion, Gram negative microorganisms are more sensitive than Gram positive bacteria to the grafted biomimetic Ag NPs.

Table 2. Microbicidal Effect (ME) of GSH Capped Silver NP Colloid, GSH-Coated Silver NP Grafted on Glass, and Uncoated Silver NP Grafted on Glass, after 5 and 24 h of Contact[a]

	contact time of GSH coated NPs colloid[b]		contact time of GSH coated NPs grafted on glass[c]		contact time of uncoated NPs grafted on glass[d]	
	5 h	24 h	5 h	24 h	5 h	24 h
cell strain	ME		ME		ME	
E. coli	1.2	3	0.42	1.38	4.93	5.90
S. aureus	0.5	1.5	0.24	0.96	1.37	5.54

[a]All values are obtained as an average of 3 experiments. ME = log N_C − log N_E (N_C is the number of CFU/mL developed on the unmodified control glasses, and N_E the number of CFU/mL counted after exposure to modified glasses; CFU = colony forming unit). [b]ref 26. [c]this work. [d]ref 33.

Considering that the surface concentration of silver, calculated from ICP-OES data, in our biomimetic-coated NPs monolayer is about 0.35 $\mu g/cm^2$, taking a 5.76 cm^2 microscope slide and 10 μL of PBS solution containing the bacteria, as used in ME experiments, we can calculate that the overall concentration of silver is about 200 $\mu g/mL$ (i.e., the concentration calculated dividing the mass of grafted silver by the total volume of the solution). In other words, during the ME experiments on GSH-coated Ag NPs grafted to the surface, the overall concentration of silver is 1 order of magnitude greater than the MIC observed for *E. coli* using dispersed NPs. Additionally, as described in the previous sections, when *E. coli* was exposed to dispersed GSH Ag NPs, the cellular damage was relevant even below the MIC. Combining these results, we can suggest that the less efficient antibacterial activity of the

dx.doi.org/10.1021/la3003838 | Langmuir 2012, 28, 8140–8148

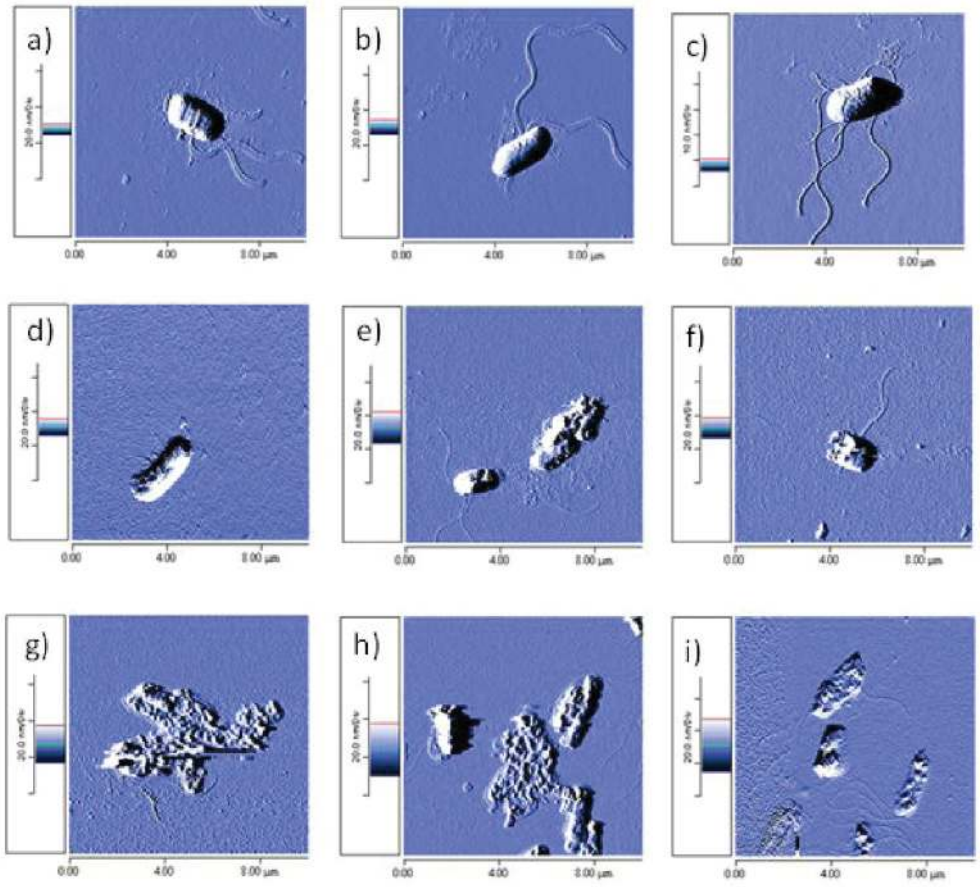

Figure 5. Representative AFM images of *E. coli* bacteria after contact for 5 h with (a,b,c) reference clean glass slides; (d,e,f) glass slides functionalized with GSH-coated Ag NPs; (g,h,i) glass slides functionalized with bare Ag NPs.

GSH-coated Ag NPs grafted to the surface might be a consequence of the restriction of translational freedom of the NPs, limiting penetration into *E. coli* cytoplasm.

On the other hand, the total amount of silver present in the monolayer is very close to the MIC previously obtained for *S. aureus*, for the dispersed colloid.[26] The greater resistance of *S. aureus* against the grafted GSH-coated Ag NPs is not surprising, considering that the relatively thicker cell wall of this Gram positive bacteria is presumably resistant enough to prevent action of Ag NPs, no matter if they are bound to a glass surface or dispersed in solution. These results can be argued as indirect evidence of a short-range mechanism of action for the antimicrobial activity of GSH coated Ag NPs.

Moreover, when the results of the ME on glass slides functionalized with GSH Ag NPs are compared (Table 2) with the ME data for glass slides bearing the Ag NPs monolayer as prepared,[33] it becomes evident that the coating with GSH of the exposed silver surface strongly reduces the antibacterial proprieties of this material. The dramatic decrease of ME is to be ascribed to the GSH coating itself, since the total amount of silver and the shape and dimensions of the NPs did not change after coating.

We investigated the release of silver ions in water from the glass slides functionalized with Ag NP monolayers coated with GSH. Samples were placed in ultrapure water and shaken for 24 h, the maximum time interval considered for the ME test used in our work. The concentration of Ag^+ in solution was measured by means of atomic absorption spectrophotometry, using a graphite-oven atomizer, and we compared these data with the Ag^+ release from the equivalent uncoated NP monolayers (i.e., in absence of GSH coating). GSH-coated Ag NPs grafted on glass released 12% (standard deviation 4%) of the total amount of silver in the monolayer, while glasses functionalized with bare NPs (i.e., in absence of GSH coating) reached a release of 14% (standard deviation 1%).[33] This evidence suggests that the antibacterial activity of grafted Ag NPs is not necessarily related to silver ion release, and that NP surface coating plays a crucial role in the interaction with bacteria coming in close contact. In other words, if Ag^+ release was the only thing responsible for the Microbicidal Effect, the value of ME should be the same in both cases (i.e., for glass samples coated with bare Ag NPs and with GSH Ag NPs).

Nevertheless, using the experimental results presented here, we can conclude that the release of ionic silver is not strongly influenced by the coating with GSH, but ME is considerably reduced after coating with GSH the surface of AgNPs grafted on glass. Moreover, one can note that the amount of silver released (12−14%) from both GSH-coated and bare Ag NPs grafted on surfaces reaches the MIC of ionic silver for *E. coli* and *S. aureus* under our experimental conditions.[26] This apparent contradiction can be explained by considering that MIC is the minimal concentration that inhibits cell proliferation, but it does not necessarily cause cell death, which is the phenomenon measured by ME tests: release of those silver ion concentrations do not strictly imply death of all bacteria present in the sample. On the other hand, one must keep in mind that, when using dispersed NPs, the amount of ionic silver released from the colloid is much lower,[26] and the

dx.doi.org/10.1021/la3003838 | *Langmuir* 2012, 28, 8140−8148

greater microbicidal effect is observed when the NPs are able to penetrate into the cytoplasm (i.e., for *E. coli*) as shown by TEM images. It is reasonable to conclude that we are observing two different processes that may concur with the overall microbicidal effects: the "long-distance" release of silver ions from the NPs and the "short-distance" nanomechanical action, involving interaction with membranes, which as expected is more intense toward Gram negative bacteria. The overall mechanism of action of both grafted and dispersed Ag NPs should be analyzed as a combination of these two processes.

AFM of *E. coli* on NPs Functionalized Glass Slides. In order to further investigate the action of the NPs grafted on the surface, we have performed AFM characterization of the interaction of *E. coli* with functionalized glass surfaces. We decided to concentrate our efforts on *E. coli*, since this microorganism shows the greater sensibility to grafted NPs,[33] and TEM data analysis revealed that internalization of NPs played an important role in their antibacterial activity against *E. coli* (see previous sections).

The procedure adopted to prepare AFM samples was similar to the experimental conditions used in ME experiments, but water was used instead of PBS, to avoid the deposition of massive material that might interfere during AFM imaging. The set of experiments includes clean glasses, glasses functionalized with bare Ag NPs, and glasses bearing the GSH-coated Ag NPs. The morphology of *E. coli* bacteria after being in contact for 5 h with clean glass slides (Figure 5a,b,c) revealed intact cells, featuring undamaged membranes and well-defined flagella. These results demonstrated that the procedure adopted to prepare the samples was not aggressive to the microorganisms.

AFM imaging of *E. coli* after 5 h in contact with glass functionalized with bare Ag NPs (Figure 5f,g,h) showed that cell membranes are completely disrupted, with evidence of cellular damage. The intracellular material has leaked and just a few cells still showed the rod-like characteristic morphology of *E. coli*, very distorted and characterized by irregular membrane surfaces. The volume of cells was considerably depressed, with respect to the control sample.

When *E. coli* was in contact with glass functionalized with biomimetically coated Ag NPs, AFM images (Figure 5d,e,f) revealed that bacterial morphology was in many cases still rod-like, and no evident intracellular material was found outside the cells. Nevertheless, cellular membranes were evidently damaged, and their surfaces were irregular, with large zones of depression.

These results can be interpreted by considering the two mechanism of action discussed in the previous section. When bacteria are exposed to glass functionalized with bare Ag NPs, the Ag^+ release mechanism and the direct nanoscale contact with silver surface are both present. The synergy of these two processes leads to generalized cell damage and causes a very strong microbicidal effect. On the other hand, when *E. coli* cells are exposed to GSH-coated NPs grafted to glass surface, Ag^+ is released, but the GSH coating presumably prevents the direct contact of cell membrane structures with Ag surfaces; therefore, cellular damage is less evident, corresponding to less intense antibacterial activity. It is not surprising that the nanomechanical contact effect produces the most dramatic damage to the cells, considering that cellular membranes contains thiol-bearing proteins and phospholipids that present high affinity for silver surfaces.[23] Indeed, when the dispersed colloid was used, TEM imaging revealed that NPs were surrounded by biological material produced by the cell (see previous sections). AFM data reinforce the hypothesis that surface features of grafted and disperse Ag NPs play a crucial role in their interaction with bacteria, modulating the mechanisms for their microbicidal effect.

CONCLUSIONS

In this work, the mechanisms of action of colloidal silver NP protected with GSH were investigated on two representative Gram positive and Gram negative bacterial strains. The effect of dispersed GSH coated Ag NPs on *Escherichia coli* is more intense and can be associated with the penetration of the colloid into the cytoplasm, with the subsequent local interaction of silver with the cell components, causing damages to the cells. For *S. aureus*, the antimicrobial effect is limited since the thick peptidoglycan layer of the cell wall prevents the penetration of the dispersed NPs inside the cytoplasm. Moreover, we showed that GSH-protected Ag NPs presented lower antibacterial activity when grafted onto functionalized glass surfaces. These GSH Ag NPs grafted on glass are also less active than the homologous bare NPs, even if the amount of Ag^+ released from the two kinds of functionalized surfaces is not strongly modified by the biocompatible coating. To interpret the data presented, the coexistence of different mechanisms already proposed in the literature[15b] should be taken into account: release of Ag^+ from NPs, and short-distance nanomechanical action, which, as expected, is more active toward Gram negative bacteria as a consequence of their less rigid membrane structure.

ASSOCIATED CONTENT

Supporting Information

TEM images of post-fixed and non-post-fixed bacteria samples at different magnifications, TEM images for quantitative analysis of the cells, AFM images of NPs functionalized glasses surfaces. This material is available free of charge via the Internet at http://pubs.acs.org.

AUTHOR INFORMATION

Corresponding Author

*E-mail: angelo.taglietti@unipv.it. Phone: +39 0382987985, fax: +39 0382 528544.

Notes

The authors declare no competing financial interest.

ACKNOWLEDGMENTS

Authors acknowledge financial support by Fondazione Cariplo (Bandi Chiusi 2007, "Superfici vetrose a azione antimicrobica basata sul rilascio modulato e controllato di cationi metallici"). J. M. Fernandez-Hechavarria and P. Pallavacini thank University of Pavia for two CICOPS Scholarships (2009 and 2011). The valuable contributions of Maria Carla Panzeri for TEM-ESI experiments (ALEMBIC, San Raffaele Scientific Institute, Milano, Italy) is also acknowledged.

REFERENCES

(1) (a) Marambio-Jones, C.; Hoek, E. M. V. A review of the antibacterial effects of silver nanomaterials and potential implications for human health and the environment. *J Nanopart. Res.* **2010**, *12*, 1531−1555. (b) Pradeep, T. A. Noble metal nanoparticles for water purification: A critical review. *Thin solid films* **2009**, *517*, 6441−6478.

(2) Morones, J. R.; Elechiguerra, J. L.; Camacho, A.; Holt, K.; Kouri, J. B.; Ramirez, J. T.; Yacaman, M. J. The bactericidal effect of silver nanoparticles. *Nanotechnology* **2005**, *16*, 2346−2353.

(3) Chaloupka, K.; Malam, Y.; Seifalian, A. M. Nanosilver as a new generation of nanoproduct in biomedical applications. *Trends Biotechnol.* **2010**, *28*, 580−588.
(4) Sondi, I.; Salopek-Sondi, B. Silver nanoparticles as antimicrobial agent: a case study on E. coli as a model for Gram-negative bacteria. *J. Colloid Interface Sci.* **2004**, *275*, 177−182.
(5) Veerapandian, M.; Yun, K. Functionalization of biomolecules on nanoparticles: specialized for antibacterial applications. *Appl. Microbiol. Biotechnol.* **2011**, *90*, 1655−1667.
(6) Rai, M.; Yadav, A.; Gade, A. Silver nanoparticles as a new generation of antimicrobials. *Biotechnol. Adv.* **2009**, *27*, 76.
(7) Kumar, A.; Vemula, P. K.; Ajayan, P. M.; John, G. Silver-nanoparticle-embedded antimicrobial paints based on vegetable oil. *Nat. Mater.* **2008**, *7*, 236.
(8) (a) Dutta, S.; Shome, A.; Kar, T.; Das, P. K. Counterion-Induced Modulation in the Antimicrobial Activity and Biocompatibility of Amphiphilic Hydrogelators: Influence of in-Situ-Synthesized Ag−Nanoparticle on the Bactericidal Property. *Langmuir* **2011**, *27*, 5000−5008. (b) El Badway, A. M.; Silva, R. G.; Morris, B.; Scheckel, K. G.; Tolaymat, T. M. Surface Charge-Dependent Toxicity of Silver Nanoparticles. *Environ. Sci. Technol.* **2011**, *45*, 283−287. (c) Neal, A. What can be inferred from bacterium−nanoparticle interactions about the potential consequences of environmental exposure to nanoparticles? *Ecotoxicology* **2008**, *17*, 362. (d) Jain, J.; Arora, S.; Rajjwade, J. M.; Omray, P.; Khandelwal, S.; Paknikar, K. M. Silver Nanoparticles in Therapeutics: Development of an Antimicrobial Gel Formulation for Topical Use. *Mol. Pharmaceutics* **2009**, *6*, 1388−1401. (e) Lee, H. Y.; Park, H. K.; Kim, K.; Park, S. B. A practical procedure for producing silver nanocoated fabric and its antibacterial evaluation for biomedical applications. *Chem. Commun.* **2007**, 2959−2961. (f) Xu, H.; Shi, X.; Ma, H.; Lv, Y.; Zhang, L.; Mao, Z. The preparation and antibacterial effects of dopa-cotton/AgNPs. *Appl. Surf. Sci.* **2011**, *257*, 6799−6803.
(9) Silver, S.; Phung, L. T.; Silver, G. Silver as biocides in burn and wound dressings and bacterial resistance to silver compounds. *J. Ind. Microbiol. Biotechnol.* **2006**, *33*, 627−634.
(10) Russell, A. D.; Hugo, W. B. Antimicrobial Activity and Action of Silver. *Prog. Med. Chem.* **1994**, *31*, 351.
(11) Chamakura, K; Perez-Ballestrero, R.; Luo, Z.; Bashir, S.; Liu, J. Comparison of bactericidal activities of silver nanoparticles with common chemical disinfectants. *Colloids Surf., B* **2011**, *84*, 88−96.
(12) Sukdeb, P.; Yu Kyung, T.; Joon Myong, S. Does the Antibacterial Activity of Silver Nanoparticles Depend on the Shape of the Nanoparticle? A Study of the Gram-Negative Bacterium Escherichia coli. *Appl. Environ. Microbiol.* **2007**, *73*, 1712−1720.
(13) (a) Shahverdi, A. R.; Fakhimi, A.; Shahverdi, H. R.; Minaian, S. Synthesis and effect of silver nanoparticles on the antibacterial activity of different antibiotics against Staphylococcus aureus and Escherichia coli. *Nanomedicine* **2007**, *3*, 168−171. (b) Sharma, V. K.; Yngard, R. A.; Lin, Y. Silver nanoparticles: Green synthesis and their antimicrobial activities. *Adv. Colloid Interface Sci.* **2009**, *145*, 83−96.
(14) (a) Silver, S. Bacterial silver resistance: molecular biology and uses and misuses of silver compounds. *FEMS Microbiol. Rev.* **2003**, *27*, 341−353. (b) Li, X. Z.; Nikaido, H.; Williams, K. E. Silver-resistant mutants of Escherichia coli display active efflux of Ag+ and are deficient in porins. *J. Bacteriol.* **1997**, *179*, 6127−6132.
(15) (a) Navarro, E.; Piccapietra, F.; Wagner, B.; Marconi, F.; Kaegi, R.; Odzak, N.; Sigg, L.; Behra, R. Toxicity of Silver Nanoparticles to Chlamydomonas reinhardtii. *Environ. Sci. Technol.* **2008**, *42*, 8959. (b) Dallas, P.; Sharma, V. K.; Zboril, R. Silver polymeric nanocomposites as advanced antimicrobial agents: Classification, synthetic paths, applications, and perspectives. *Adv. Colloid Interface Sci.* **2011**, *166*, 119−135.
(16) Dror-Ehre, A.; Mamane, H.; Belenkova, T.; Markovich, G.; Adin, A. Silver nanoparticle−E. coli colloidal interaction in water and effect on E. coli survival. *J. Colloid Interface Sci.* **2009**, *339*, 521−526.
(17) Zhang, Y.; Peng, H.; Huang, W.; Zhou, Y.; Yan, D. Facile preparation and characterization of highly antimicrobial colloid Ag or Au nanoparticles. *J. Colloid Interface Sci.* **2008**, *325*, 371−376.
(18) Feng, Q. L.; Wu, J.; Chen, G. Q.; Cui, F. Z.; Kim, T. N.; Kim, J. O. A mechanistic study of the antibacterial effect of silver ions on Escherichia coli and Staphylococcus aureus. *J. Biomed. Mater. Res.* **2000**, *52*, 662−668.
(19) Wu, J.; Hou, S. Y.; Ren, D. C.; Mather, P. T. Antimicrobial Properties of Nanostructured Hydrogel Webs Containing Silver. *Biomacromolecules* **2009**, *10*, 2686−2693.
(20) Holt, K. B.; Bard, A. J. Interaction of Silver(I) Ions with the Respiratory Chain of Escherichia coli: An Electrochemical and Scanning Electrochemical Microscopy Study of the Antimicrobial Mechanism of Micromolar Ag+. *Biochemistry* **2005**, *44*, 13214−13223.
(21) Wigginton, N. S.; De Titta, A.; Piccapietra, F.; Dobias, J.; Neasatyy, V. J.; Suter, M. J. F.; Bernier-Latmani, R. Binding of Silver Nanoparticles to Bacterial Proteins Depends on Surface Modifications and Inhibits Enzymatic Activity. *Environ. Sci. Technol.* **2010**, *44*, 2163−2168.
(22) Xu, X.-H. N.; Brownlow, W. J.; Kyriacou, S. V.; Wan, Q.; Viola, J. J. Real-Time Probing of Membrane Transport in Living Microbial Cells Using Single Nanoparticle Optics and Living Cell Imaging. *Biochemistry* **2004**, *43*, 10400.
(23) (a) Li, W.; Xie, X.; Shi, Q.; Zeng, H.; OU-Yang, Y.; Chen, Y. Antibacterial activity and mechanism of silver nanoparticles on Escherichia coli. *Appl. Microbiol. Biotechnol.* **2010**, *85*, 1115. (b) Li, W.-R.; Xie, X.-B.; Shi, Q.-S.; Duan, S.-S.; Ouyang, Y.-S.; Chen, Y.-B. Antibacterial effect of silver nanoparticles on Staphylococcus aureus. *Biometals* **2011**, *24*, 135−141.
(24) Yamanaka, M.; Hara, K.; Kudo, J. Bactericidal Actions of a Silver Ion Solution on Escherichia coli, Studied by Energy-Filtering Transmission Electron Microscopy and Proteomic Analysis. *Appl. Environ. Microbiol.* **2005**, *71*, 7589−7593.
(25) Singh, S.; Patel, P.; Jaiswal, S.; Prabhune, A. A.; Ramana, C. V.; Prasad, B. L. V. A direct method for the preparation of glycolipid−metal nanoparticle conjugates: sophorolipids as reducing and capping agents for the synthesis of water re-dispersible silver nanoparticles and their antibacterial activity. *New J. Chem.* **2009**, *33*, 646−652.
(26) Amato, E.; Diaz-Fernandez, Y. A.; Taglietti, A.; Pallavicini, P.; Pasotti, L.; Cucca, L.; Milanese, C.; Grisoli, P.; Dacarro, C.; Fernandez-Hechavarria, J. M.; Necchi, V. Synthesis, Characterization and Antibacterial Activity against Gram Positive and Gram Negative Bacteria of Biomimetically Coated Silver Nanoparticles. *Langmuir* **2011**, *27*, 9165−9173.
(27) (a) Frederix, F.; Friedt, J. M.; Choi, K. H.; Laureyn, W.; Campitelli, A.; Mondelaers, D.; Maes, G.; Borghs, G. Biosensing Based on Light Absorption of Nanoscaled Gold and Silver Particles. *Anal. Chem.* **2003**, *75*, 6894−690. (b) Tripathy, S. J.; Yu, Y. T. Spectroscopic investigation of S−Ag interaction in ω-mercaptoundecanoic acid capped silver nanoparticles. *Spectrochim. Acta, Part A* **2009**, *72*, 841−844.
(28) Wu, Q.; Cao, H.; Luan, Q.; Zhang, J.; Wang, Z.; Warner, J. H.; Watt, A. A. R. Biomolecule-Assisted Synthesis of Water-Soluble Silver Nanoparticles and Their Biomedical Applications. *Inorg. Chem.* **2008**, *47*, 5882.
(29) Slocik, J.; Wright, D. Biomimetic Mineralization of Noble Metal Nanoclusters. *Biomacromolecules* **2003**, *4*, 1135.
(30) Mandal, S.; Gole, A.; Lala, N.; Gonnade, R.; Ganvir, V.; Sastry, M. Studies on the Reversible Aggregation of Cysteine-Capped Colloidal Silver Particles Interconnected via Hydrogen Bonds. *Langmuir* **2001**, *17*, 6262−6268.
(31) Martínez-Castañón, G. A.; Niño-Martínez, N.; Martínez-Gutierrez, F.; Martínez-Mendoza, J. R.; Ruiz, F. Synthesis and antibacterial activity of silver nanoparticles with different sizes. *J. Nanopart. Res.* **2008**, *10*, 1343−1348.
(32) Panacek, A.; Kvitek, L.; Prucek, R.; Kolar, M.; Vecerova, R.; Pizurova, N.; Sharma, V. K.; Nevecna, T.; Zboril, R. Silver Colloid Nanoparticles: Synthesis, Characterization, and Their Antibacterial Activity. *J. Phys. Chem. B* **2006**, *110*, 16248.
(33) Pallavicini, P.; Taglietti, A.; Dacarro, G.; Diaz Fernandez, Y. A.; Galli, M.; Grisoli, P.; Patrini, M.; Santucci De Magistris, G.; Zanoni, R. Self-assembled monolayers of silver nanoparticles firmly grafted on

glass surfaces: Low Ag+ release for an efficient antibacterial activity. *J. Colloid Interface Sci.* **2010**, *350*, 110.
(34) Pallavicini, P.; Dacarro, G.; Cucca, L.; Denat, F.; Grisoli, P.; Patrini, M.; Sok, N.; Taglietti, A. A monolayer of a Cu2+-tetraazamacrocyclic complex on glass as the adhesive layer for silver nanoparticles grafting, in the preparation of surface-active antibacterial materials. *New J. Chem.* **2011**, *35*, 1198−1201.
(35) (a) Danese, P. N. Antibiofilm Approaches: Prevention of Catheter Colonization. *Chem. Biol.* **2002**, *9*, 873. (b) Lewis, K.; Klibanov, A. M. Surpassing nature: rational design of sterile-surface materials. *Trends Biotechnol.* **2005**, *23*, 343. (c) Simchi, A.; Tamjid, E.; Pishbin, F.; Boccaccini, A. R. Recent progress in inorganic and composite coatings with bactericidal capability for orthopaedic applications. *Nanomedicine: NBM* **2011**, *7*, 22. (d) Costerton, J. W.; Montanaro, L.; Arciola, C. R. Biofilm in implant infections: Its production and regulation. *Int. J. Artif. Organs* **2005**, *28*, 1062−1068. (e) Arciola, C. R.; Montanaro, L.; Costerton, J. W. New trends in diagnosis and control strategies for implant infections. *Int. J. Artif. Organs* **2011**, *34*, 727−736.
(36) (a) Burda, C.; Chen, X.; Narayanan, R.; El-Sayed, M. A. Chemistry and Properties of Nanocrystals of Different Shapes. *Chem. Rev.* **2005**, *105*, 1025−1102. (b) Xia, Y.; Halas, N. J. Shape-Controlled Synthesis and Surface Plasmonic Properties of Metallic Nanostructures. *MRS Bull.* **2005**, *30*, 338−348. (c) Moores, A.; Goettmann, F. The plasmon band in noble metal nanoparticles: an introduction to theory and applications. *New J. Chem.* **2006**, *30*, 1121−1132. (d) Evanoff, D. D., Jr.; Chumanov, G. Synthesis and Optical Properties of Silver Nanoparticles and Arrays. *ChemPhysChem* **2005**, *6*, 1221−1231. (e) Wiley, B.; Sun, Y.; Xia, Y. Synthesis of Silver Nanostructures with Controlled Shapes and Properties. *Acc. Chem. Res.* **2007**, *40*, 1067−1076. (f) Ghosh, S. K.; Nath, S.; Kundu, S.; Esumi, K.; Pal, T. Solvent and Ligand Effects on the Localized Surface Plasmon Resonance (LSPR) of Gold Colloids. *J. Phys. Chem. B* **2004**, *108*, 13963−13971. (g) Stewart, M. E.; Anderton, C. R.; Thompson, L. B.; Maria, J.; Gray, S. K.; Rogers, J. A.; Nuzzo, R. G. Nanostructured Plasmonic Sensors. *Chem. Rev.* **2008**, *108*, 494−521.
(37) NCCLS, Methods for dilution antimicrobial susceptibility tests for bacteria that grow aerobically, in *Approved Standard M7-A6*, 6th ed., Wayne, PA, 2003.
(38) Franke, W. W.; Krien, S.; Brown, R. M., Jr. Simultaneous glutaraldehyde-osmium tetroxide fixation with postosmication. *Histochem.Cell Biol.* **1969**, *19*, 162−164.
(39) Pezzati, R.; Bossi, M.; Podini, P.; Meldolesi, J.; Grohovaz, F. High-resolution calcium mapping of the endoplasmic reticulum-Golgi-exocytic membrane system. Electron energy loss imaging analysis of quick frozen-freeze dried PC12 cells. *Mol. Biol. Cell* **1997**, *8*, 1501−1512.